# Di-ureasil ormolytes doped with $Mg^{2+}$ ions.

# Part 1: Morphological, thermal and electrochemical properties

**S. C. Nunes[a], V. de Zea Bermudez[a]*, M. M. Silva[b], S. Barros, M. J. Smith[b], E. Morales[c], L. D. Carlos[d], J. Rocha[e]**

[a]*Departamento de Química and CQ-VR, Universidade de Trás-os-Montes e Alto Douro, 5000-911 Vila Real, Portugal*

[b]*Departamento de Química, Universidade do Minho, Gualtar,* 4710-057 *Braga, Portugal*

[c]*Instituto de Ciencia y Tecnología de Polímeros (CSIC), Calle Juan de la Cierva 3, 28006 Madrid, Spain*

[d]*Departamento de Física and CICECO, Universidade de Aveiro, 3810-193 Aveiro, Portugal*

[e]*Departamento de Química and CICECO, Universidade de Aveiro, 3810-193 Aveiro, Portugal*

**Abstract**

Poly(oxyethylene) (POE)/siloxane-based materials incorporating magnesium triflate ($Mg(CF_3SO_3)_2$) were synthesized by the sol-gel process. The host Class II hybrid matrix (di-ureasil) employed is composed of a siliceous framework to which short POE chains are covalently bonded through urea linkages. Ormolytes with salt composition n (molar ratio of oxyethylene moieties per $Mg^{2+}$ ion) ranging from ∞ to 1 were investigated. The nanohybrid with n = 20, which is thermally stable up to 360 ºC, exhibits the highest conductivity (e.g., approximately $4.0 \times 10^{-6}$ and $6.7 \times 10^{-5}$ $\Omega^{-1}cm^{-1}$ at 35 and 104 ºC, respectively). The redox stability domain of this material spans from -3.0 to +2.0 V versus $Mg/Mg^{2+}$.

**Keywords:** sol-gel, di-ureasil, magnesium triflate, complex impedance, cyclic voltammetry

* Corresponding author. Tel: +351-259-350253; Fax: +351-259-350480.

E-mail address: vbermude@utad.pt

## 1. Introduction

Since 1983, when the results reported by Bertier et al. [1] suggested that the ionic conductivity in semi-crystalline polymer electrolytes (PEs) was confined to the amorphous phase, the attention of researchers in this domain has been directed towards the preparation of essentially amorphous host materials based on poly(oxyethylene) (POE)-based macromolecules [2]. Recent results reported by Gadjourova et al. [3] are in conflict with this accepted model, and indicate that ion transport may also occur in the crystalline region of the polymer network and, under certain circumstances, this contribution to the total conductivity may be greater than that of the amorphous component. Nevertheless, as the levels of conductivity displayed by the electrolytes prepared by Gadjourova et al.[3] are still too low to foresee any immediate technological application, much of the work carried out at present continues to be focused on the development of amorphous systems.

The synthesis of hybrid structures is of interest in this context. POE/siloxane frameworks incorporating ionic salts have attracted much attention over the last decades, because of their potential application as electrolytes in solid state electrochemical devices, and particularly in advanced lithium batteries [4-13]. The development of such organic/inorganic structures permits, not only a significant reduction or even suppression of crystallinity, but may also result in a marked improvement in the mechanical resistance and the chemical/thermal stability of the materials. In addition, POE/siloxane host matrices are able to solubilize greater quantities of guest salts than conventional macromolecules, avoiding "salting-out". Thin and flexible ormolyte (organically modified silicate electrolyte) films are readily produced through the sol-gel process [14]. Two types of hybrids may be produced [13]: Class I hybrids, in which weak interactions (van der Waals contacts, hydrogen bonding or electrostatic interactions) are established between both components (one acts as host network and the other as entrapped species), and Class II hybrids, in which at least a proportion of the organic and

inorganic components are bonded by means of strong chemical interactions (covalent or iono-covalent bonds).

The number of studies of electrolytes containing $Mg^{2+}$ ions is relatively limited. Some Pes [15-22] and gel polymer electrolytes (GPEs) [23-26] incorporating magnesium salts have been characterized. The synthesis of $Mg^{2+}$-doped ormolytes prepared via sol-gel has only been reported quite recently by Mitra and Sampath [27]. These authors describe a Class I matrix derived from tetraethoxyortosilane and poly(ethylene glycol) to which magnesium perchlorate and magnesium chloride were added [27].

The development of $Mg^{2+}$-based systems assume significant importance in solid state electrochemistry. With an electrode potential of -2.37 V versus SHE and an electrochemical equivalence of 2.2 $Ahg^{-1}$, Mg is an attractive anode material [28]. The use of Mg for the fabrication of rechargeable solid state batteries looks also very promising [29]: (1) its natural abundance makes it cheaper than Li; (2) it is non-toxic and thus environmentally friendly; (3) it is less reactive than Li towards oxygen and humid atmospheres and thus hazards in open air are minimized; (4) the ionic radii of $Li^+$ and $Mg^{2+}$ are comparable in magnitude, meaning that magnesium batteries may use insertion compounds which have been developed for lithium cells.

In the present work we will investigate POE/siloxane ormolytes doped with magnesium triflate ($Mg(CF_3SO_3)_2$). The host structure of these materials - which contains POE chains with approximately 40.5 repeat units - belongs to the class of *di-ureasils* [30-32], a family of Class II hybrids in which the organic and inorganic components are bonded through urea groups. This study will be divided into two parts: Part 1 will be devoted to the synthesis and characterization of the structure, morphology, thermal properties and electrochemical behaviour of a series of di-ureasil xerogels with a wide range of $Mg(CF_3SO_3)_2$ concentration; in Part 2[33] an in-depth infrared and Raman spectroscopic analysis of the same set of samples

will be reported to characterize the local cation and anion environments and explain the dependence of the ionic conductivity with salt content.

## 2. Experimental Details

### 2.1. Materials

Magnesium trifluoromethanesulfonate ($Mg(CF_3SO_3)_2$, Aldrich) and α,β-diaminepoly(oxyethylene-co-oxypropylene (commercially designated by Jeffamine ED-2001®, Fluka, average molecular weight 2001 g/mol) were dried under vacuum at 25 ºC for several days prior to being used. 3-isocyanatepropyltrietoxisilane (ICPTES, Fluka) was used as received. Ethanol (Merck) and tetrahydrofuran (Merck) were stored over molecular sieves. High purity distilled water was used in all experiments.

### 2.2. Synthesis

The $Mg^{2+}$-based di-ureasils were prepared according to the method described in detail elsewhere for the $Eu^{3+}$ [34,35]- and $Li^+$ [12]-based analogues. Globally, the synthetic procedure involved grafting a POE-based diamine to the isocyanatepropyltriethoxysilane precursor, to yield the di-urea cross-linked hybrid precursor molecule,

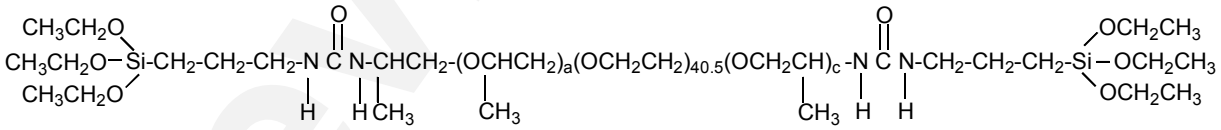

a+c = 2.5

which was subsequently hydrolyzed and condensed in the sol-gel stage to induce the growth of the siloxane network.

In agreement with the terminology adopted in previous publications [12,34,35], the ormolytes were identified using the notation d-U(2000)$_n$$Mg(CF_3SO_3)_2$, where d-U(2000) represents the host di-ureasil framework (d stands for di, U denotes the urea group and 2000

corresponds to the average molecular weight of the starting organic precursor) and n (salt composition) indicates the number of ether oxygen atoms per $Mg^{2+}$cation. For example, the di-ureasil xerogel d-U(2000)$_{20}$Mg($CF_3SO_3$)$_2$ contains an amount of Mg($CF_3SO_3$)$_2$ such that the $O_{POE}$ /$Mg^{2+}$ molar ratio is equal to 20.

The content of Mg($CF_3SO_3$)$_2$ in the samples and other relevant information is given in Table 1. The xerogels with n > 1 were obtained as transparent, flexible monoliths with a yellowish hue, whereas the material with n = 1 is a white solid.

### 2.3. Experimental techniques

**NMR.** $^{29}$Si magic-angle spinning (MAS) and $^{13}$C cross-polarization (CP) MAS NMR spectra were recorded on a Brüker Avance 400 (9.4 T) spectrometer at 79.49 and 100.62 MHz, respectively. $^{29}$Si MAS NMR spectra were recorded with 2 μs (equivalent to 30 º) rf pulses, a recycle delay of 60 s and at a 5.0 kHz spinning rate. $^{13}$C CP/MAS NMR spectra were recorded with 4 μs $^1$H 90º pulse, 2 ms contact time, a recycle delay of 4 s and at a spinning rate of 8 kHz. Chemical shifts (δ) are quoted in ppm from TMS.

**XRD**. The X-ray diffraction (XRD) measurements were performed at room temperature (RT) with a Rigaku Geigerflex D/max-c diffractometer system using monochromated $CuK_\alpha$ radiation (λ = 1.54 Å) over the 2θ range of between 4 and 80 º at a resolution of 0.05 º. The xerogel samples, analyzed as films, were not submitted to any thermal pre-treatment.

**DSC and ATG.** A DSC131 Setaram Differential Scanning Calorimeter was used to determine the thermal characteristics of the ormolytes. Disk sections with masses of approximately 30 mg were removed from the di-ureasil film, placed in 40 μl aluminium cans and stored in a dessicator over phosphorous pentoxide ($P_2O_5$) for one week at RT under vacuum. In the case of the di-ureasil with n = 1 it was necessary to grind the sample first to form a fine powder in order to remove all the water. After the drying treatment the cans were hermetically sealed

and the thermograms were recorded. Each sample was heated from 25 to 300 ºC at 10 ºC $min^{-1}$. It was subsequently quenched from RT to -100 ºC and then heated up to 80 ºC at 15 ºC $min^{-1}$. The purge gas used in both experiments was high purity nitrogen supplied at a constant 35 $cm^3$ $min^{-1}$ flow rate. Samples for thermogravimetric studies were transferred to open platinum crucibles and analysed using a Rheometric Scientific TG 1000 thermobalance (materials with n = 200, 7, 5 e 1) and a Mettler TGA/SDTA 851 thermobalance (materials with n = 60, 40 and 20) at a heating rate of 10º $min^{-1}$ using dried nitrogen as purging gas (20 ml/min). Prior to measurement, the xerogels were vacuum-dried at 80 ºC for about 48 h and kept in an argon-filled glove box.

**Complex impedance.** For bulk conductivity measurements, an ormolyte disk was placed between two 10 mm diameter ion-blocking gold electrodes (Goodfellow, > 99.9%). The electrode/ormolyte/electrode assembly was secured in a suitable constant volume support. The cell support was installed in a Buchi TO51 tube oven and a type K thermocouple placed close to the electrolyte disk measured the sample temperature. Bulk conductivities of the samples were obtained during heating cycles using the complex plane impedance technique (Schlumberger Solartron 1250 frequency response analyser and 1286 electrochemical interface) over a temperature range of between 25 and 100 ºC and at approximately 7 ºC intervals. Prior to characterization, the di-ureasil ormolytes were vacuum-dried at 80 ºC for about 48 h and kept in an argon-filled glove box.

**Cyclic Voltammetry**. Cyclic voltammetry measurements were performed at RT in an argon-filled glove box using a Radiometer Voltalab 32 potentiostat/galvanostat equipment operating at a 10 $mVs^{-1}$ scan rate in the potential range of -4.0 to 4.0 V versus $Mg/Mg^{2+}$. The PE sample was sandwiched between two low-carbon stainless steel (SS) ion blocking electrodes, with a Mg foil as negative electrode, and located inside a PTFE sealed test cell. The electrode area was 0.283 $cm^2$. Prior to characterisation, the ormolyte sample was dried under vacuum at 60 ºC for about 24 hours.

# 3. Results and Discussion

## 3.1. Structure and Morphology

The $^{29}$Si MAS and $^{13}$C CP/MAS NMR spectra of selected d-U(2000)$_n$Mg($CF_3SO_3$)$_2$ ormolytes are reproduced in Figs. 1(a) and 1(b), respectively. The position and attribution [12,36-46] of the resonance peaks are listed in Table 2.

The $^{29}$Si MAS NMR spectra of the d-U(2000)$_n$Mg($CF_3SO_3$)$_2$ xerogels with n = 80, 20 and 10 exhibit three signals at *ca.* -52, -58 and -66 ppm (Fig. 1(a)). On the basis of the conventional $T_m$ silicon (Si) notation (m = 1, 2 and 3, where m* is the number of Si atoms bonded to O-Si units), these peaks are ascribed, respectively, to $T_1$ ($CH_2$-Si(OR)$_2$(OSi)), $T_2$ ($CH_2$-Si(OR)(OSi)$_2$) and $T_3$ ($CH_2$-Si(OSi)$_3$) sites, where R is $CH_2CH_3$ or H (Table 2). The calculated relative population for the three Si environments confirms that in both samples the sites present are essentially $T_3$ (close to 60%) and $T_2$ (almost 40%) (Table 2), suggesting a branched nature for the polycondensed structures. This result correlates well with the magnitude of the polycondensation rates c (where c = 1/3 (%$T_1$ + 2%$T_2$ + 3%$T_3$)) derived for the same $Mg^{2+}$-doped di-ureasils (around 86%), which are significantly higher than the value reported for the non-doped framework (75%) [46]. The empirical formula deduced for the three d-U(2000)$_n$Mg($CF_3SO_3$)$_2$ $Mg^{2+}$-doped nanohybrids (Table 2) indicates that a minor number of $OCH_2CH_3$ or OH groups persist attached to the Si atoms.

The most significant feature of the $^{13}$C CP/MAS NMR spectra of the di-ureasils with n = 80, 20 and 10 represented in Fig.1(b) is a peak at about 70 ppm, attributed to the resonance of the dominating $OCH_2CH_2O$ moieties of d-U(2000) (Table 2). The remaining functional groups of this hybrid matrix, which are considerably less abundant, give rise to very weak signals (Fig.1(b)). We note that the urea C=O resonance expected at 160 ppm appears as a weak event in the spectra of the Mg($CF_3SO_3$)$_2$-doped composites (insert of Fig.1(b)). As

* The classical notation $T_n$ has been changed to $T_m$, to avoid any confusion with the notation n used for salt composition throughout the text.

demonstrated in Table 2, the $^{13}C$ CP/MAS NMR data confirm that the grafting reaction gave rise to the formation of the urea group and was not accompanied by the rupture of bonds in the Si-propyl segments or oligopolymer groups. In agreement with the conclusions drawn from the $^{29}Si$ MAS NMR data, the $^{13}C$ CP/MAS NMR spectra support the suggestion that the hydrolysis reaction was incomplete, as unreacted $OCH_2CH_3$ groups remain in the materials.

Close analysis of the XRD patterns of the d-U(2000)$_n$Mg(CF$_3$SO$_3$)$_2$ samples illustrated in Fig. 2 allows us to conclude that the composites with n = 40, 20 and 10 are totally amorphous, those with n ≥ 60 are semi-crystalline, whereas the most concentrated sample (n = 1) is crystalline. These findings demonstrate that, in contrast with the situation found in the $Li^+$-containing system [12], the addition of a considerable amount of guest salt to the d-U(2000) medium is needed to inhibit the formation of crystalline phases of pure POE or POE/salt complexes or free Mg(CF$_3$SO$_3$)$_2$. The broad band, Gaussian in shape, centered at approximately 21.61º in the diffractograms of materials with 200 ≥ n ≥ 5 is associated with the coherent diffracting domains of the siliceous backbone [47]. The application of Bragg's law permits us to conclude that the structural unit distance is approximately 4.22 Å. The sharp and intense peaks detected at about 19.15 and 23.25 º in the diffractograms of the doped di-ureasils with 200 ≥ n ≥ 60 are produced by crystalline POE domains (Fig. 2) [47]. The salt-rich material d-U(2000)$_1$Mg(CF$_3$SO$_3$)$_2$ gives rise to a series of well-defined peaks which do not correspond to the characteristic peaks of Mg(CF$_3$SO$_3$)$_2$ (Fig. 2). This result induces us to propose that a crystalline POE/Mg(CF$_3$SO$_3$)$_2$ complex is formed at this salt concentration. On the basis of a previous study of the conventional POE$_n$Mg(CF$_3$SO$_3$)$_2$ system [20], we feel tempted to further suggest that the stoichiometry of the crystalline compound found in the d-U(2000) medium is 8. We will seek in Part 2 of this series of papers [33] spectroscopic evidences of the formation of this POE/Mg(CF$_3$SO$_3$)$_2$ complex in the d-U(2000) medium.

The DSC curves of the d-U(2000)$_n$Mg($CF_3SO_3$)$_2$ nanohybrids represented in Fig. 3(a) corroborate the XRD data: only the samples with $40 \geq n \geq 10$ give rise to thermograms typical of amorphous materials. The pair of low temperature, weak melting peaks visible in the DSC traces of the di-ureasils with $200 \geq n \geq 60$ (Fig. 3(a)) substantiate the presence of a minor component of crystalline POE domains [34]. The origin of the series of endotherms found between 100 and 200 ºC in the DSC curves of the xerogels with n = 5 (weak and broad) and 1 (well resolved and strong) is uncertain. They might be associated with the fusion of the POE/Mg($CF_3SO_3$)$_2$ complex identified by means of XRD and with degradation reactions. Acosta and Morales [20] showed that the crystalline $POE_8Mg(CF_3SO_3)_2$ complex melts at 214 ºC. As the POE chains of d-U(2000) are significantly shorter than those of the POE employed by the above authors ($5x10^6$ $gmol^{-1}$ [20]), the melting temperature of the complex occurring in the ormolyte material is expected to be much lower. We will return to the discussion of these thermal events below.

Valuable information regarding the coordination of the cations to the host macromolecule in PE systems may be also retrieved from DSC experiments. As this interaction restricts the local motion of polymer chains, an increase of the glass temperature ($T_g$), that may be monitored in the thermograms, results.[2] The variation of the $T_g$ of the d-U(2000)$_n$Mg($CF_3SO_3$)$_2$ electrolytes with composition, represented in Fig. 3(b), clearly shows that the $T_g$ of the POE chains of d-U(2000) (-54 ºC) [12] remains practically unaffected by the inclusion of increasing amounts of guest salt in samples with $n \geq 60$. This strongly suggests that either the POE chains of the di-ureasil matrix do not bond to the $Mg^+$ ions within this salt composition range or the number of cross-links between the guest species and the POE chains of the d-U(2000) matrix is insufficient to alter the physical behaviour of the polymer within this range of concentration. The further incorporation of guest salt (n = 40 and 20) leads, however, to a slight $T_g$ rise (Fig. 3(b)), an indication that in both samples the alkaline-earth

ions interact with the ether oxygen atoms of the polymer segments. The $T_g$ upshift is particularly dramatic at higher salt concentration (about 36 and 55 ºC, at n = 10 and 5, respectively). The role of the polyether chains in the coordination process of the cations in the d-U(2000)$_n$Mg($CF_3SO_3$)$_2$ hybrids will be one of the main issues to be investigated in Part 2 [33].

The TGA curves of representative d-U(2000)$_n$Mg($CF_3SO_3$)$_2$ di-ureasils are depicted in Fig. 4. Samples with $200 \geq n \geq 20$ undergo a single weight loss. Close analysis of the ATG curves of the more diluted composites lead us to conclude that Mg($CF_3SO_3$)$_2$ exerts a remarkable stabilizing effect on d-U(2000). While the non-doped matrix starts to decompose at about 305 ºC [12], the di-ureasils with n = 60, 40 and 20 are thermally stable up to 361 ºC (Fig. 4). In the case of the salt-rich compounds with $7 \geq n \geq 1$ degradation takes place in three stages: a slight weight loss (around 10%) occurs at about 52 ºC, that proceeds with two abrupt changes at about 310 and 440 ºC (Fig. 4). It is noteworthy that the major degradation of the most concentrated di-ureasil examined (n = 1) occurs in the third stage (Fig. 4). These data allow us to assign the endotherms evident in the DSC thermograms of the hybrids with n = 5 and 1 to the coupled effect of thermal decomposition and fusion of the crystalline $POE_8Mg(CF_3SO_3)_2$ complex.

### 3.2. Ionic conductivity and electrochemical stability

The most appropriate salts for POE-type PEs are those which have low lattice energy, i.e., salts consisting of a polarizing cation and a large anion of delocalized charge, requiring little solvation [2]. The $Mg^{2+}$ ion and the hard $CF_3SO_3^-$ base used in the present work fulfil these requirements. Nevertheless, while strong cation-polymer bonds are necessary for PE formation, labile bonds are essential for cation mobility. Thus, in principle diffusion of a divalent cation in POE would be expected to be impeded. A comparison of the cation transference numbers of POE-based PEs doped with metallic cations and the water exchange

rates around the aqueous cations suggests that $Mg^{2+}$ is an immobile ion [2]. Consequently, PEs based on magnesium salts should be essentially anionic conductors.

The examination of the Arrhenius conductivity plots of the $Mg^{2+}$-doped ormolytes with n ≥ 5 illustrated in Fig. 5(a) reveals that above 25 ºC the most conducting ormolyte is d-U(2000)$_{20}$Mg(CF$_3$SO$_3$)$_2$. This amorphous compound exhibits 4.0x10$^{-6}$, 1.0x10$^{-5}$ and 6.74x10$^{-5}$ $\Omega^{-1}$cm$^{-1}$ at 35, 50 and 104 ºC, respectively. At n = 5 a marked reduction in conductivity is observed (Fig. 5(a)). The graph of the conductivity isotherms shown in Fig. 5(b) confirms that the conductivity maximum of this di-ureasil system appears distinctly at n = 20.

It is of interest to determine whether the modification of the POE architecture carried out in the present work by means of the hybrid approach is beneficial from the standpoint of ionic conductivity.

Let us first compare the results obtained here with those reported in the literature for improved PEs doped with the same magnesium salt The only value found in the literature for the conventional POE$_n$Mg(CF$_3$SO$_3$)$_2$ system relates to the sample with n = 8 [20]. As this sample corresponds to a crystalline complex, it conducts poorly (e.g., 3.21x10$^{-8}$ $\Omega^{-1}$cm$^{-1}$ at 50 ºC)[20] and consequently cannot be used for the purpose of comparison. As expected, the ambient temperature conductivity displayed by the d-U(2000)$_{20}$Mg(CF$_3$SO$_3$)$_2$ maximum is significantly lower than that exhibited by other systems proposed previously: (1) electrolyte samples composed of Mg(CF$_3$SO$_3$)$_2$, propylene carbonate (PC) and ethylene carbonate (EC) included in a photo-cross-linked polymer of poly(ethylene glycol) diacrylate reinforced by a porous propylene membrane (1.7x10$^{-4}$ $\Omega^{-1}$cm$^{-1}$ at 25 ºC for 1%mol of Mg(CF$_3$SO$_3$)$_2$)[21]; (2) POE$_8$Mg(CF$_3$SO$_3$)$_2$ plasticized with PC, EC and a mixture of PC and EC (approximately 1x10$^{-3}$ $\Omega^{-1}$cm$^{-1}$ at 20 ºC)[22]; (3) GPEs consisting of polyacrylonitrile (PAN), PC, EC and Mg(CF$_3$SO$_3$)$_2$ (1.8x10$^{-3}$ $\Omega^{-1}$cm$^{-1}$ at 20 ºC for an optimal molar PAN:PC:EC:Mg(CF$_3$SO$_3$)$_2$ ratio of 1:2:2:0.4) [24]; (4) Mg(CF$_3$SO$_3$)$_2$-doped GPEs based on poly(methylmethacrylate)

(PMMA) plasticized with PC and EC ($4.2x10^{-4}$ $\Omega^{-1}cm^{-1}$ at 20 ºC for an optimal molar PMMA:(PC+EC):$Mg(CF_3SO_3)_2$ ratio of 1:2:0.5) [26].

As the nature of the anion is known to have a major influence on ionic conductivity it is important to examine the levels of conductivity attained with other magnesium salts. Patrick et al. [15] doped POE with magnesium perchlorate ($Mg(ClO_4)_2$) and found that the conductivity of the electrolyte with n = 12 was approximately $5x10^{-7}$ $\Omega^{-1}cm^{-1}$at 20 ºC. The electrolytes prepared with POE and magnesium chloride ($MgCl_2$) by Yang et al. [16,17] exhibit very poor conductivity at RT (between $10^{-10}$ and $10^{-9}$ $\Omega^{-1}cm^{-1}$). More recently, a RT conductivity of ca. $1.9x10^{-5}$ $\Omega^{-1}cm^{-1}$ was reported for complexes synthesized from a low molecular weight poly(ethylene glycol) and a highly crystallographic disordered form of $MgCl_2$ (designated as δ-$MgCl_2$) [19]. We should also comment the only previously published results describing the ionic conductivity of sol-gel derived $Mg^{2+}$-doped electrolytes [27]. At RT the most conducting Class I ormolytes of Mitra and Sampath [27] attain $10^{-7}$ and $10^{-5}$ $\Omega^{-1}cm^{-1}$ in the presence of $MgCl_2$ and $Mg(ClO_4)_2$, respectively.

We note that the conduction mechanism in the hybrid di-urea cross-linked medium will probably be substantially different from that occurring in the conventional POE-based matrix. In fact, while in the di-ureasil host structure two types of coordinating locations (the ether oxygen atoms and the carbonyl oxygen atoms) may be active, in the latter situation only the ether oxygen atoms have the ability to solvate the cations. The identification of the mobile species in the d-U(2000)-based ormolytes will be the objective of Part 2 of this series of papers [33].

The cyclic voltamogram of the amorphous d-$U(2000)_{20}Mg(CF_3SO_3)_2$ xerogel is reproduced in Fig. 6. The electrochemical stability window is limited on the anodic side by the irreversible oxidation of the $CF_3SO_3^-$ ion. In this voltammogram an obvious increase in the current density occurs at potentials higher than +1.0 V vs. $Mg/Mg^{2+}$, similar to the

situation observed with a GPE of PMMA doped with $Mg(CF_3SO_3)_2$ and plasticized with PC and EC [26]. However it should be also stressed that the measured current density values are very low (of the order of $10^{-2}$ $\mu Acm^{-2}$), suggesting that the di-ureasil ormolyte with n = 20 can be considered electrochemically stable over a wide potential range (from approximately -3.0 to +2.0 V versus $Mg/Mg^{2+}$).

## 4. Conclusion

Poly(oxyethylene) (POE)/siloxane-based materials incorporating magnesium triflate ($Mg(CF_3SO_3)_2$) were synthesized by the sol-gel process. The host Class II hybrid matrix (di-ureasil) employed is composed of a siliceous framework to which short POE chains are covalently bonded through urea linkages. Ormolyte films with $\infty > n \geq 1$ (where n, salt composition, is the molar ratio of oxyethylene moieties per $Mg^{2+}$ ion) were studied. While materials with $n \geq 60$ contain crystalline POE regions, xerogels with $40 \geq n \geq 10$ are entirely amorphous. At n = 1 a crystalline POE/$Mg(CF_3SO_3)_2$ complex is formed. Samples with $200 > n \geq 20$ are thermally stable up to 360 ºC. The nanohybrid with n = 20 exhibits the highest conductivity (approximately $4.0x10^{-6}$ and $6.7x10^{-5}$ $\Omega^{-1}cm^{-1}$ at 35 and 104 ºC, respectively). The electrochemical stability domain of this hybrid spans approximately 5 V (from -3.0 to +2.0 V versus $Mg/Mg^{2+}$).

The encouraging results obtained with the d-$U(2000)_nMg(CF_3SO_3)_2$ materials, specially the improved mechanical properties and the moderate ionic conductivity, induce us to state that further research on $Mg^{2+}$-doped d-U(2000)-based di-ureasils is worth pursuing. The incorporation of a more suitable magnesium salt instead of $Mg(CF_3SO_3)_2$ will certainly yield materials with higher ionic conductivity values.

## 5. Acknowledgement

This work was supported by Fundação para a Ciência e Tecnologia (POCTI/P/CTM/33653/00, SFRH/BD/13559/03 and POCTI/P/CTM/46780/03). S. C. Nunes acknowledges Fundação para a Ciência e Tecnologia for a grant.

## 6. References

1. C. Berthier, W. Gorecki, M. Minier, M. B. Armand, J. M. Chabagno and P. Rigaud, *Solid State Ionics* **11** (1983), p. 91.

2. F. M. Gray, Polymer Electrolytes, RSC Materials Monographs, The Royal Society of Chemistry, London, 1997.

3. Z. Gadjourova, Y. G. Andreev, D. P. Tunstall and P. G. Bruce, *Nature* **412** (2001), p. 520.

4. D. Ravaine, M. Armand, Y. Charbouillot and N. Vincens, *J. Non-Cryst. Solids* **82** (1986), p. 210.

5. M. Popall, M. Andrei, J. Kappel, J. Kron, K. Olma and B. Olsowski, *Electrochim. Acta* **43 (10-11)** (1998), p. 1155.

6. P. Judeinstein, J. Titman, M. Stamm and H. Schmidt, *Chem. Mater*. **6** (1994), p. 127.

7. K. Dahmouche, M. Atik, N. C. Mello, T. J. Bonagamba, H. Panepucci, M. A. Aegerter and P. Judeinstein, *J. Sol-Gel Sci. Technol*. **8** (1997), p. 711.

8. V. de Zea Bermudez, L. Alcácer, J. L. Acosta and E. Morales, *Solid State Ionics* **116** (1999), p. 197.

9. C. Wang, Y. Wei, G. R. Ferment, W. Li and T. Li, *Mater. Lett*. **39** (1999), p. 206.

10. J. R. MacCallum and S. Seth, *Eur. Polym. J*. **36** (2000), p. 2337.

11. K. Nishio and T. Tsuchiya, *Sol. Energy Mater. Sol. Cells* **68** (2001), p. 295.

12. S. C. Nunes, V. De Zea Bermudez, D. Ostrovskii, M. M. Silva, S. Barros, M. J. Smith, L. D. Carlos, J. Rocha and E. Morales, *J. Electrochem. Soc*., **152(2)** (2005), p. xxx

13. Functional Hybrid Materials, P. Gomez-Romero and C. Sanchez, Editors, Wiley Interscience, New York, 2003

14. C. J. Brinker and G. W. Scherer, Sol-gel Science: The Physics and Chemistry of Sol-Gel Processing, Academic Press, San Diego, CA, 1990

15. A. Patrick, M. Glasse, R. Latham and R. Linford, *Solid State Ionics* **18&19** (1986), p. 1063.

16. L. L. Yang, A. R. McGhie and G. C. Farrington, *J. Electrochem. Soc*. **133(1)** (1986), p. 1380.

17. L. L. Yang, R. Huq, G. C. Farrington and G. Chiodelli, *Solid State Ionics* **18 & 19** (1986), p. 291.

18. G. C. Farrington, in *Polymer Electrolyte Reviews 2*, J. R. MacCallum and C. A. Vincent (Eds), Elsevier Science Publishers, 1989, chapter 8

19. V. Di Noto, S. Savina, D. Longo and M. Vidali, *Electrochim. Acta* **43(10-11)** (1998), p. 1225.

20. J. L. Acosta and E. Morales, *Electrochim. Acta* **43 (7)** (1998), p. 791.

21. S. Ikeda, Y. Mori, Y. Furuhashi and H. Masuda, *Solid State Ionics* **121** (1999), p. 329.

22. G. Girish Kumar and N. Munichandraiah, *J. Electroanal. Chem* **495** (2000), p. 42.

23. G. Girish Kumar and N. Munichandraiah, *Electrochim. Acta* **44** (1999), p. 2663.

24. G. Girish Kumar and N. Munichandraiah, *Solid State Ionics* **128** (2000), p. 203.

25. G. Girish Kumar and N. Munichandraiah, *J. Power Sources* **91**(2000), p. 157.

26. G. Girish Kumar and N. Munichandraiah*, Electrochim. Acta* **47**(2002), p. 1013.

27. S. Mitra and S. Sampath, *J. Mater. Chem.* **12** (2002), p. 2531.

28. J. L. Robinson, in *The Primary Battery*, N. C. Cahoon, G. W. Heise (Eds), volume II, John Wiley, 1976, p. 149.

29. D. Aurbach, Z. Lu, A. Schechter, Y. Gofer, H. Gizbar, R. Turgeman, Y. Cohen, M. Moshkovich and E. Levi, *Nature* **407** (2000), p. 724.

30. M. Armand, C. Poinsignon, J.-Y. Sanchez and V. de Zea Bermudez, U.S. Patent 5, 283, 310, 1993

31. V. de Zea Bermudez, C. Poinsignon and M. B. Armand*, J. Mater. Chem*. **7(9)** (1997), p. 1677.

32. V. de Zea Bermudez, D. Baril, J.-Y. Sanchez, M. Armand and C. Poinsignon, A. Hugot-Le Goff, C.- G. Granqvist and C. M. Lampert, (Eds), Proc. SPIE, 1992, Vol. 1728, 180

33. S. C. Nunes, V. de Zea Bermudez, D. Ostrovskii and L. D. Carlos, *This Journal*, submitted.

34. M. M Silva, V. de Zea Bermudez, L. D. Carlos, A. P. Passos de Almeida and M. J. Smith, *J. Mater. Chem*. **9** (1999), p. 1735.

35. M. M. Silva, V. de Zea Bermudez, L. D. Carlos and M. J. Smith, *Electrochim. Acta* **45** (2000), p. 1467.

36. P. Judeinstein, J. Titman, M. Stamm and H. Schmidt, *Chem. Mater*. **6** (1994), p. 127.

37. F. Ribot, A. Lafuma, C. Eychenne-Baron and C. Sanchez, *Adv. Mater.* **14** (2002), p. 1496.

38. D. Cohn, A. Sosnik and A. Levy, *Biomater*. **24** (2003), p. 3707.

39. M. C. Gonçalves, V. de Zea Bermudez, R. A. Sá Ferreira, L. D. Carlos, D. Ostrovskii and J. Rocha, *Chem. Mater*.16(13) (2004), p. 2530-2543

40. S. R. Davis, A. R. Brough and A. Atkinson, *J. Non-Cryst. Solids* **315** (2003), p. 197.

41. A.-C. Franville, D. Zambon, R. Mahiou and Y. Troin, *Chem. Mater.* **12** (2000), p. 428.

42. T. C. Chang, G. P. Wang, H. C. Tsai, Y. S. Hong and Y. S. Chiu, *Polym. Degrad. Stab.* **74** (2001), p. 229.

43. E. El Nahhal, M. M. Chehimi, C. Cordier and G. Dodin, *J. Non-Cryst. Solids* **275** (2000), p. 142.

44. S. Hvidt, E. B. Jørgersen, W. Brown and K. Schillén, *J. Phys. Chem*. **98** (1994), p. 12320.

45. E. A. Williams, C. L. Sabourin, P. E. Donahue, J. L. Spivack and N. A. Marotta, General Electric Research & Development Center, Technical Information Series (98CRD171), Dec. 1998.

46. L. D. Carlos, R. A. Sá Ferreira, I. Orion, V. de Zea Bermudez and J. Rocha, *J. Lumin.* **87-89** (2000), p. 702.

47. L. D. Carlos, V. de Zea Bermudez, R. A. Sá Ferreira, L. Marques and M. Assunção, *Chem. Mater*. **11(3)** (1999), p. 581.



 

## List of figure captions

Fig. 1 - $^{29}$Si MAS (a) and $^{13}$C CP/MAS (b) NMR spectra of selected d-U(2000)$_n$Mg($CF_3SO_3$)$_2$ di-ureasils

Fig. 2 - XRD patterns of the d-U(2000)$_n$Mg($CF_3SO_3$)$_2$ di-ureasils

Fig. 3 - Thermal behaviour of the d-U(2000)$_n$Mg($CF_3SO_3$)$_2$ di-ureasils: (a) DSC thermograms; (b) Glass transition temperature versus composition.

Fig. 4 - TGA curves of selected d-U(2000)$_n$Mg($CF_3SO_3$)$_2$ di-ureasils.

Fig. 5 - Arrhenius conductivity plot (a) and isotherms of the ionic conductivity vs. composition (b) of the d-U(2000)$_n$Mg($CF_3SO_3$)$_2$ di-ureasils

Fig. 6 - Room temperature cyclic voltamogram of the d-U(2000)$_{20}$Mg($CF_3SO_3$)$_2$ di-ureasil (5$^{th}$ cycle, sweep rate = 10 mV $s^{-1}$) obtained with a SS/ormolyte/Mg/SS cell.

### Tables

Table 1 - Details of the synthetic procedure of the d-U(2000)$_n$Mg($CF_3SO_3$)$_2$ di-ureasils

Table 2 - $^{29}$Si MAS/NMR and $^{13}$C CP/MAS data (in ppm) of selected d-U(2000)$_n$Mg($CF_3SO_3$)$_2$ di-ureasils

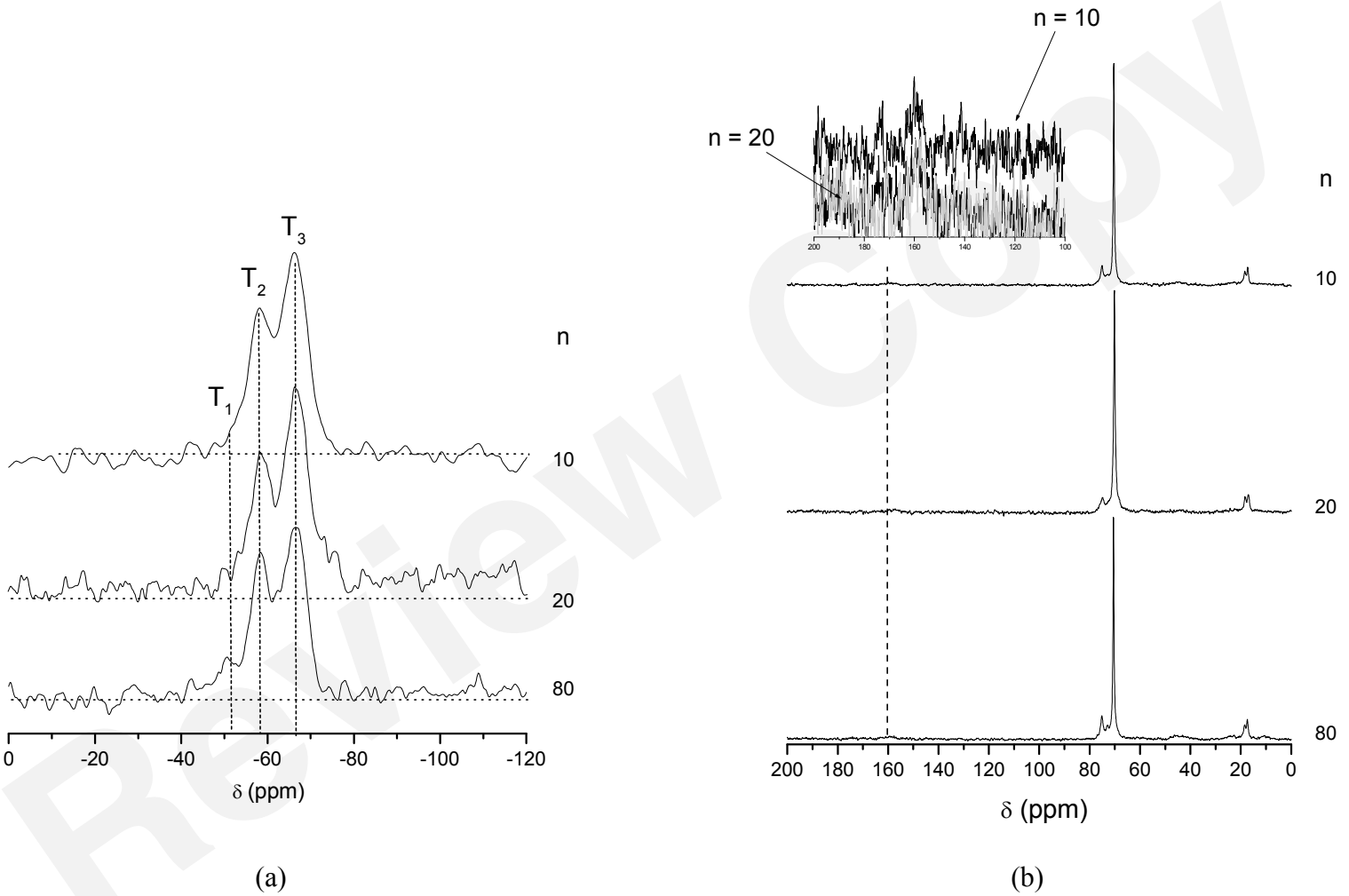


(a) (b)

Fig. 1, S. C. Nunes et al., *Solid State Ionics*

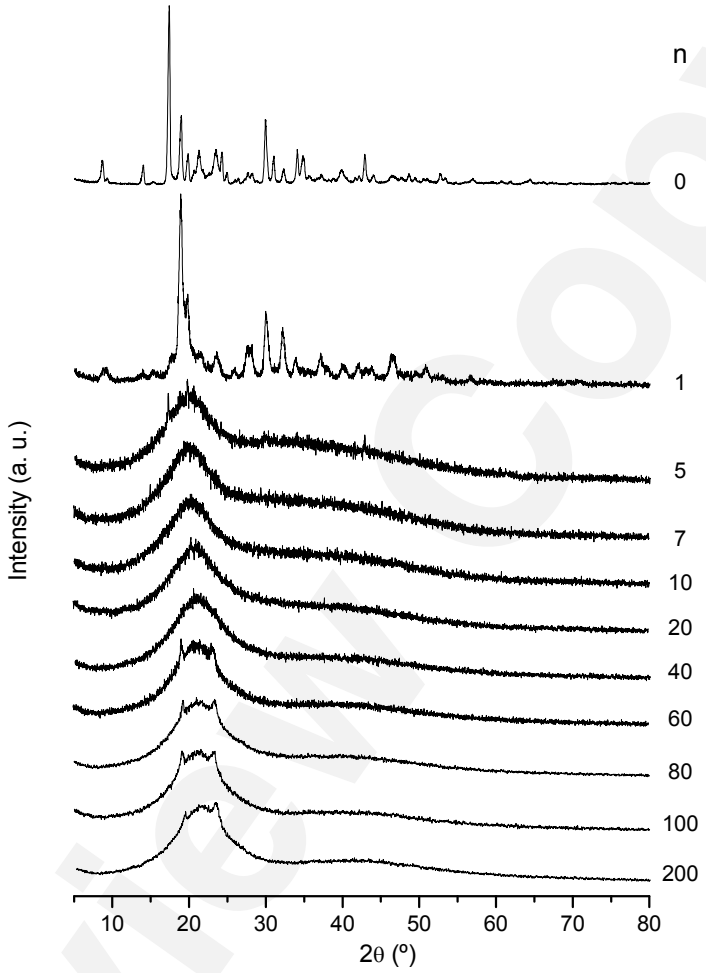


Fig. 2, S. C. Nunes et al., *Solid State Ionics*

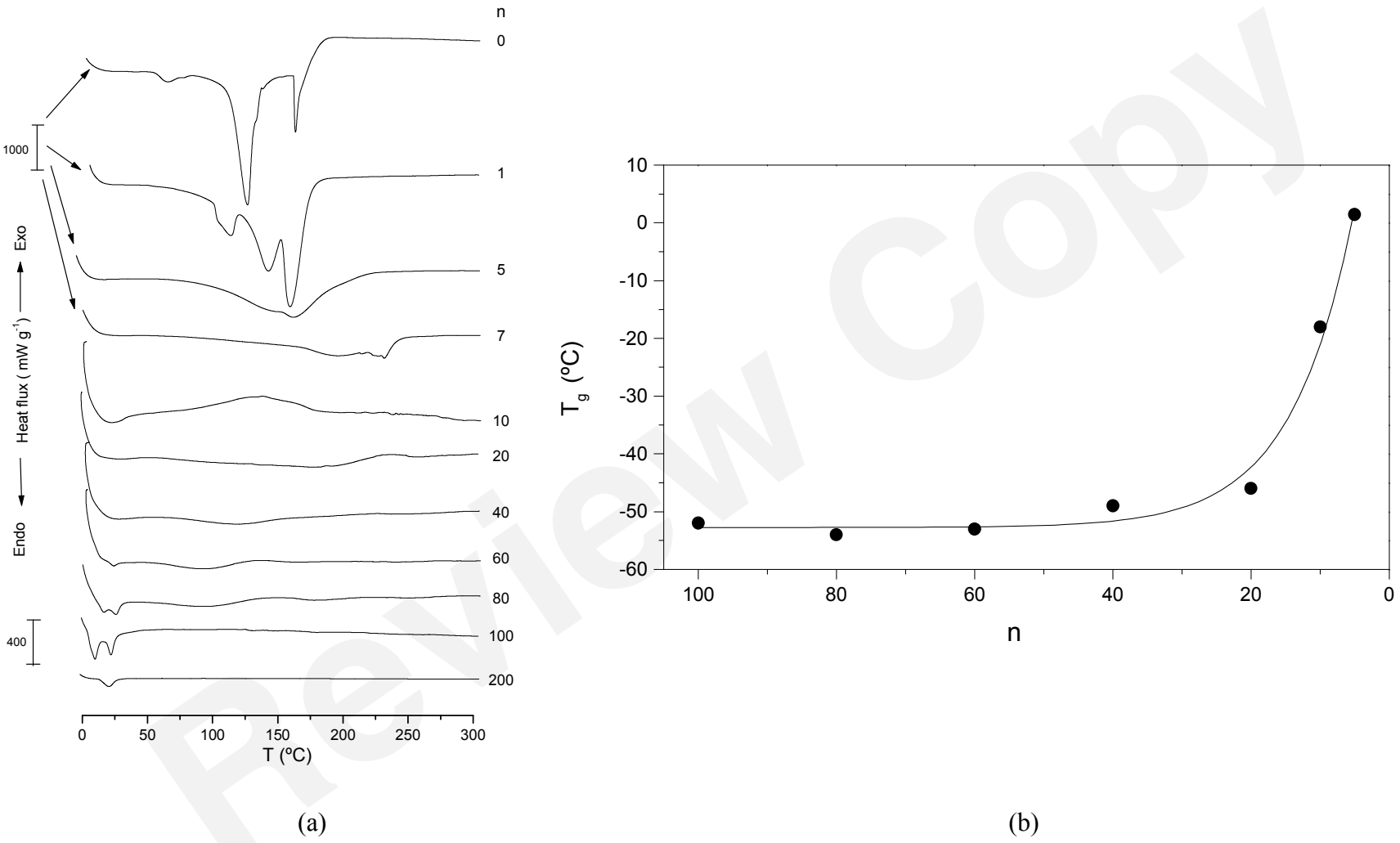


Fig. 3, S. C. Nunes et al., *Solid State Ionics*

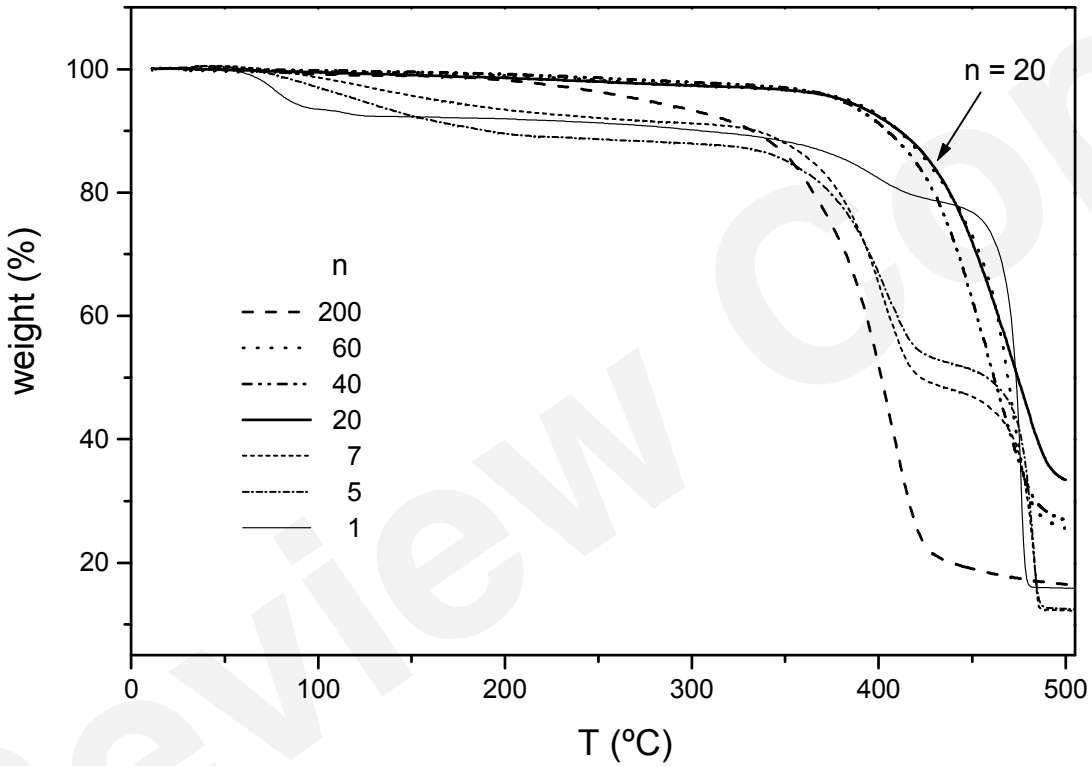


Fig. 4, S. C. Nunes et al., *Solid State Ionics*

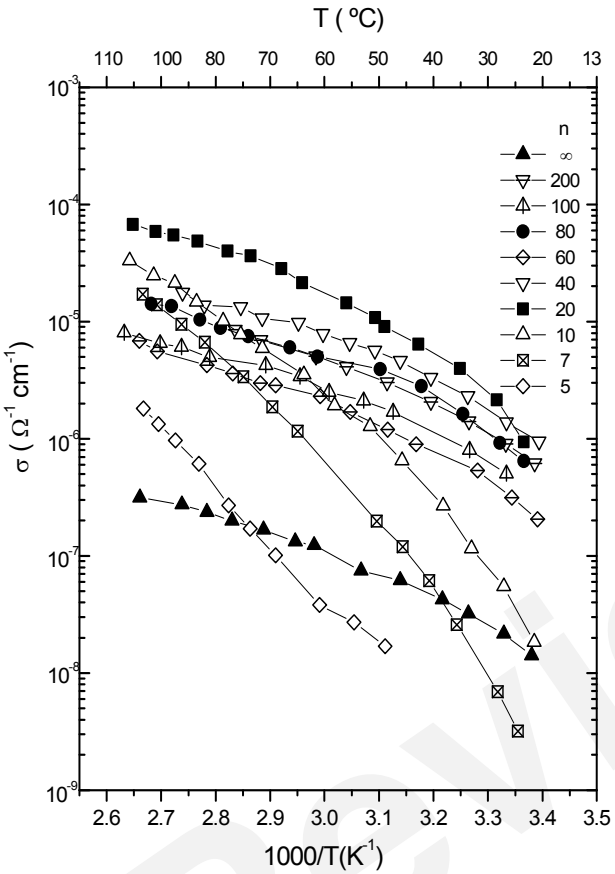


(a)

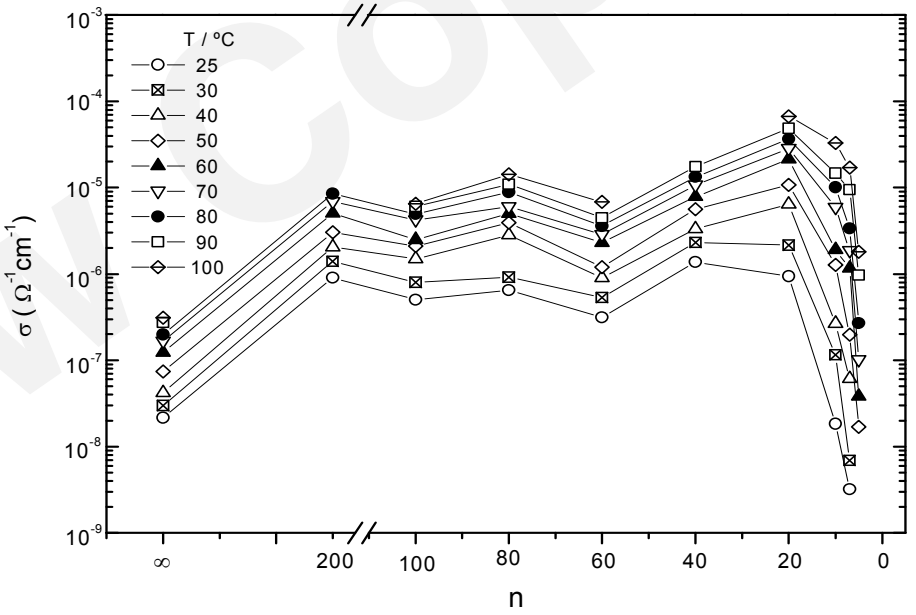


(b)

Fig. 5, S. C. Nunes et al., *Solid State Ionics*

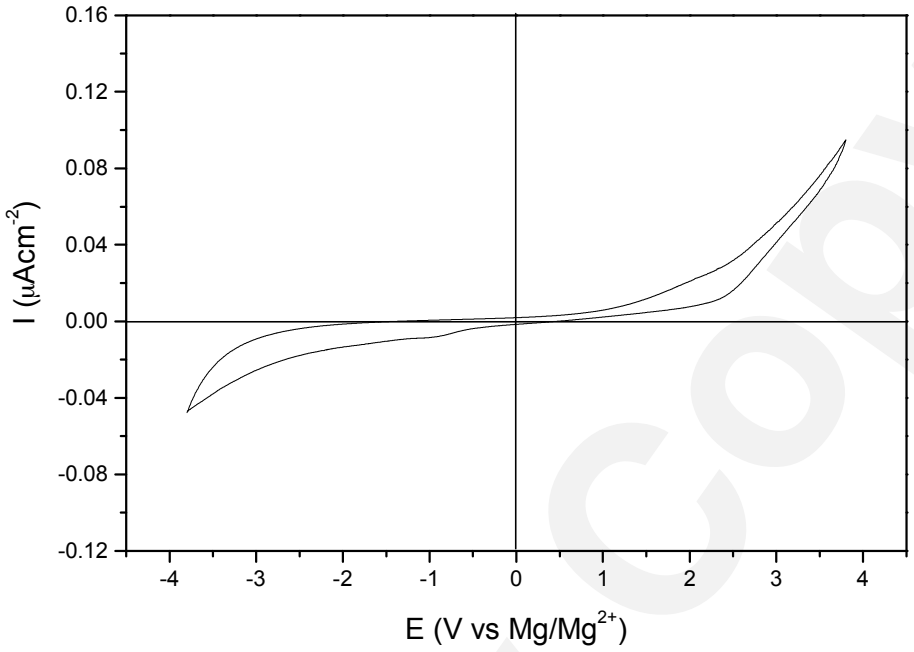


Fig. 6, S. C. Nunes et al., *Solid State Ionics*

Table 1, S. C. Nunes et al., *Solid State Ionics*

| $n = O/Mg^{2+}$ ($molmol^{-1}$) | $m(Mg(CF_3SO_3)_2)$ (g) | $Si/Mg^{2+}$ ($molmol^{-1}$) | $Si/Mg^{2+}$ ($gg^{-1}$) |
|---|---|---|---|
| ∞ | - | - | - |
| 200 | 0.0816 | 9.8765 | 7.5769 |
| 100 | 0.1632 | 4.9383 | 3.7884 |
| 80 | 0.2040 | 3.9506 | 3.0307 |
| 60 | 0.2721 | 2.9630 | 2.2728 |
| 40 | 0.4081 | 1.9753 | 1.5154 |
| 20 | 0.8162 | 0.9876 | 0.7577 |
| 10 | 1.6324 | 0.4938 | 0.3788 |
| 5 | 3.2648 | 0.2469 | 0.1894 |
| 1 | 16.324 | 0.0494 | 0.0379 |

Table 2, S. C. Nunes et al., *Solid State Ionics*

| $^{29}$Si MAS | | | | | | | | |
|---|---|---|---|---|---|---|---|---|
| n | $T_1$ ($CH_2$-Si(OSi)$(OR)_2$) | population (%) | $T_2$ ($CH_2$-Si$(OSi)_2(OR)$) | population (%) | $T_3$ ($CH_2$-Si$(OSi)_3$) | population (%) | c (%) | Empirical formula |
| 80 | -51.0 | 2.0 | -58.5 | 39.1 | -66.3 | 59.0 | 86 | $R'_{0.5}Si\ (OR)_{0.45}(O)_{1.3}$ |
| 20 | -53.4 | 2.1 | -58.5 | 38.9 | -66.4 | 58.9 | 85 | $R'_{0.5}Si\ (OR)_{0.45}(O)_{1.3}$ |
| 10 | -52.0 | 1.8 | -58.0 | 36.3 | -66.0 | 61.9 | 87 | $R'_{0.5}Si\ (OR)_{0.40}(O)_{1.3}$ |

| $^{13}$C CP/MAS | | | | |
|---|---|---|---|---|
| n | | | | Attribution[12] |
| ∞ | 80 | 20 | 10 | |
| 160 | | | | C=O |
| 75 | 75.2 | 74.9 | 75.1 | O**C**$H_2$**C**H($CH_3$) |
| 72-70 | 70.6 | 70.2 | 70.4 | O**C**$H_2$**C**$H_2$O |
| 61 | - | - | - | O**C**$H_2CH_3$ |
| 47-41 | - | - | - | **C**$H_2CH_2CH_2Si$ |
| 25-22 | - | - | - | **C**$H_2CH_2Si$ |
| 18 | 18.4 | 18.3 | 18.4 | OC$H_2$**C**$H_3$ |
| 17 | 17.4 | 17.0 | 17.3 | OC$H_2$CH(**C**$H_3$) |
| 15-10 | - | - | - | **C**$H_2Si$ |

Note: R'= -$(CH_2)_3$-NH-C(=O)-NH-(CH($CH_3$)$CH_2$-(OCH($CH_3$)$CH_2)_a$-$(OCH_2CH_2)_{40.5}$-(OCH($CH_3$)$CH_2)_b$-NH-C(=O)-NH-$(CH_2)_3$-

R = H ou $CH_2CH_3$